

Mechanical and Thermal Expansion Properties of Wood-PVC/LDPE Nanocomposite

Mohammadreza Beygi, Saied Nouri Khorasani*, Parisa Kamalian, Mohadeseh Najafi, and Shahla Khalili

Department of Chemical Engineering, Isfahan University of Technology, Isfahan 84156-83111, Iran

(Received August 15, 2021; Revised November 27, 2021; Accepted December 9, 2021)

Abstract: In the present research, mechanical properties, water absorption, and thermal stability of wood-poly(vinyl chloride)/low-density polyethylene (wood-PVC/LDPE) composite were improved via nanoclay addition. The presence of LDPE and Cloisite 30B at variable contents was studied. The composites were prepared by melt compounding and then compression molding. The morphology, mechanical, physical, and thermal properties of the composites were investigated. The micrographs of scanning electron microscopy (SEM) confirmed an appropriate coherence existing between lignocelluloses filler and PVC/LDPE matrix. The results revealed that the composite with 30 phr (parts per hundred) LDPE showed the best impact strength as 2887.33 kJ/m². Besides, adding 3 phr nanoclay to the composite improved the impact strength by about 14 % and decreased the water absorption by 61 % compared to the PVC/wood composite. Also, the linear thermal expansion coefficient of the nanocomposite was 4.5×10^{-5} 1/°C. The X-ray diffraction (XRD) pattern reflected that exfoliated structure was developed in the optimum compound. The obtained results recommended that the optimum properties could be attained using LDPE of 30 phr and 3 phr Cloisite 30B in the wood-PVC composite.

Keywords: Poly(vinyl chloride), Low-density polyethylene, Cloisite 30B, Thermal expansion, Mechanical properties

Introduction

Nowadays, one of the concerns about human societies is environmental pollution. Using natural materials is known as the most important strategy for reducing the environmental pollution. Natural fibers and wood are renewable offers to operate as biodegradable reinforcing materials for synthetic polymers. The addition of these materials to the polymers is interested due to their low density, high strength, extensive availability, no abrasiveness, and low cost [1-4]. However, the hydrophilic structure of wood fibers makes them incompatible with the polymers, which is the main reason for non-uniform dispersion and thereby poor stress transfer between the wood particles and polymer matrix [5-7]. The addition of coupling agents such as silane coupling agents and maleic anhydride-grafted-polymer is an appropriate method to tackle this problem and improve the interfacial adhesion between the filler and polymer matrix [8-11]. Coupling agents open up an opportunity for the formation of chemical bonds with OH groups of the wood fibers. Besides, coupling agents can reduce the hydrophilicity of the wood fibers with the elimination of available and free hydrophilic OH groups of cellulosic materials [12,13].

Several types of research have been done in developing wood-plastic composites (WPCs) in various applications. Poly(vinyl chloride) is known as the most commonly used polymer matrix for WPCs, which has high tensile strength, chemical resistance, polarity, and reasonable price [14,15]. However, because of the low impact strength along with high water absorption of this composite, using PE with high hydrophobicity can improve these weaknesses. Thongpin *et*

al. reported that the presence of 10 phr HDPE to PVC polymer without any compatibilizer leads to a reduction of the young module, and impact strength of the blend. Besides, by increasing the amount of HDPE to 30 phr, the impact strength was noticeably reduced [16]. Similar results were observed by Xu *et al.* in PVC/LDPE blends in the absorbance of compatibilizer, which is due to poor surface adhesion between the two polymers [17]. It was worth mentioning that adding a greater amount of wood sawdust as a biodegradable reinforcing material instead of polymer phase without considerable changes in mechanical properties could be beneficial to industries along with the environment and thereby cost-saving [5,18].

The addition of a compatibilizer to the blend can improve the interfacial adhesion, and therefore develop the mechanical properties [19-22]. One of the suitable compatibilizers in the PVC/LDPE blend in the presence of wood is PA20, which is composed of poly(methyl methacrylate-co-butyl acrylate) along with the long vinyl chains. Formation of dipole-dipole interaction between methyl methacrylate, and butyl acrylate molecules with the PVC phase, along with compatibility of vinyl chains with LDPE, can improve the adhesion between the PVC and LDPE [13]. Prachayawarakorn *et al.* considered the effect of three various types of compatibilizers, including chlorinated polyethylene (CPE), poly(methyl methacrylate-co-butyl acrylate), and poly(ethylene-co-methacrylate) (Elvaloyon) along with rubber-wood sawdust content on the mechanical properties of PVC/LDPE composite. They explained that using 15 % of the poly(methyl methacrylate-co-butyl acrylate) compatibilizer greatly enhanced the mechanical properties of the composite [5].

In another study, they reported that adding three %wt. MAPE, as a coupling agent, in PVC/LDPE with a constant

*Corresponding author: saied@iut.ac.ir

amount of wood and poly(methyl methacrylate-co-butyl acrylate), causes desirable mechanical properties [13].

These days, nanoclay caught the attention of several researchers because of showing significant development in the properties of WPCs. Nanoclays are layered silicates with transportable ions between these layers. The use of hard nanoparticles dramatically increases the thermal and mechanical properties of the composite. Considerable attempts have been made toward improving mechanical properties and thermal stability by employing the nanoclay [23-25]. Zhao *et al.* investigated the effect of modified wood and montmorillonite clay on the physical and mechanical properties of the PVC/Wood composite. They concluded that modification of the wood floor with 1.5 phr silane increased the tensile and impact strengths, and the addition of amine-modified nanoclay considerably enhanced the fire flame retardancy along with smoke suppression [26]. In other research, Broysiak *et al.* showed increasing in the waste and storage modulus of PP/wood/nanoclay composite with the growth of nanoclay content from 1 to 3 phr [27]. Deka *et al.* reported that the behavior of the PE/PP/PVC composite in the presence of wood particles depends on nanoclay content, which was modified by amine groups [28].

According to previous studies, no significant change in mechanical properties of the PVC/LDPE composites was seen with increasing the amount of wood sawdust up to 50 phr [18]. Therefore, the aim of this paper is to investigate the effect of greater sawdust content (60 phr) on the mechanical properties of PVC/LDPE composite for producing an economical and environmentally friendly composite. However, the problem of increasing the thermal expansion coefficient of the composite due to the addition of polyethylene still exists. Improving the mechanical properties of wood-PVC/LDPE composite along with the reduction of the thermal expansion coefficient with nanoclay has not been investigated yet. This study focused on detecting the optimum percentage of PE and nanoclay in the wood-PVC/LDPE composite. The poly(methyl-methacrylate-co-butyl acrylate) as a compatibilizer and coupling agent of maleic anhydride-grafted-polyethylene (MAPE) were used to improve compatibility between LDPE and PVC blend. The morphology, mechanical properties, water absorption, and thermal properties of the wood-PVC/LDPE blend containing 0 to 4 phr nanoclay were determined.

Experimental

Materials

A suspension grade of poly(vinyl chloride) (PVC, S6558, K Value=65), and low-density polyethylene (LDPE) with LF0200 commercial name (MFI=2 g/10 min⁻¹) were supplied by Bandar Imam Petrochemical Co. (Iran). The Cloisite® 30B, as a modified nanoclay, was purchased from Southern Clay Co. (USA). The applied coupling agent was maleic

anhydride-grafted-polyethylene (MAPE), provided by Kimia Javid Esfahan Co. (Iran). Poly(methyl methacrylate-co-butyl acrylate) (PA910) as a compatibilizer was provided from LG Co. Wood particles were obtained from the beech tree, was sieved with the standard of 60-80 mesh, which is corresponding to the particle size of 170-250 μm. The thermal stabilizer (GH124), impact modifier (IM812), and plasticizer (DOP) were provided by Kimiaran Co., LG Co., and AEK Yung Co., respectively.

Sample Preparation

Firstly, PVC (100 phr), wood particles (60 phr), DOP (1 phr), compatibilizer (6 phr), thermal stabilizer (5 phr), and impact modifier (6 phr) were mixed in an internal mixer for 5 min at 120 °C. The mixture was then extruded in a counter-rotating twin-screw extruder (SJZ65/132 model, china) with a screw diameter of 65 cm, and *l/d* ratio of 17.4, and a screw speed of 15-20 rpm. The thermal profile was varied from 170 to 180 °C. The produced granules were compounded in a co-rotating twin-screw extruder (TE-35C) with different amounts of LDPE (10, 20, 30, and 40 phr), and nanoclay (1, 2, 3, and 4 phr) as reported in Table 1. The MAPE granules were also added in this stage as a constant value of 1.8 phr. The screw diameter and the *l/d* ratio were 3506 cm, and 32, respectively. All the compounds were molded by a compression molding machine using a temperature of 200 °C for 8 min for further experiments.

Sample Characterization

The interfacial morphology of the wood-PVC/LDPE composites was studied using scanning electron microscopy (FE-SEM, Quanta™ 450 FEG, Philips, Germany). The prepared samples with compression molding were immersed in a nitrogen liquid for 10 minutes and were broken. Before the morphological studies, the samples were gold coated.

The wide-angle X-ray diffraction analysis (XRD) was done using the X-pert Philips diffractometer (Netherlands), to investigate the intercalated morphology of the nanoclay in

Table 1. Code and composition of the prepared samples

Sample code	PVC (phr)	Wood particles (phr)	LDPE (phr)	MAPE (phr)	Cloisite 30B (phr)
R	100	60	0	0	0
L10	100	60	10	1.8	0
L20	100	60	20	1.8	0
L30	100	60	30	1.8	0
L40	100	60	40	1.8	0
L30N1	100	60	30	1.8	1
L30N2	100	60	30	1.8	2
L30N3	100	60	30	1.8	3
L30N4	100	60	30	1.8	4

the composites. The applied beam of the XRD was Cu K α ($\lambda=1.541$ nm), with 40 kV and 30 mA. The scanning rate and 2θ ranges were 1 °C/min and 0.5-10 °, respectively.

The tensile experiments were performed according to ASTM D638 at a crosshead speed of 1 mm·min⁻¹, and a gauge length of 25.4 mm. The type V dumbbell specimens were prepared by CNC according to the standard. For each compound, the average values and standard deviations from three replicates were reported.

The Izod pendulum impact tests were performed according to ASTM D256 on the prepared samples with a deep v-shaped gap at three replicates.

The water absorption test was performed according to ASTM D570-98. All samples were placed at 50 °C for 24 hours and then were dried in a vacuum oven at 105 °C for one hour. After that, the dried samples were weighed (M_{dry}), and completely submerged in distilled water at room temperature for 24 hours. The samples were taken out and weighed again (M_{wet}). The percentage of water absorption was calculated after 24 hours from equation (1).

$$\% \text{ Water absorption} = \left[\frac{(M_{wet} - M_{dry})}{M_{dry}} \right] \times 100 \quad (1)$$

The linear dimensional stability of the compounds was investigated using the linear thermal expansion coefficient. A vertical line with a specified length of L_1 was drawn on each specimen at 23 °C (T_1). Then, all samples were retained in an oven for 48 h at 60 °C (T_2). After removing the specimen from the oven, the drawn line was measured with an accuracy of 0.01 mm (L_2). Samples were then placed in a freezer at -18 °C for 48 h (T_3), and the length of the line was accurately measured (L_3). The linear thermal expansion coefficient of the samples was calculated from equation (2).

$$k = \left(\frac{1}{L_1} \right) m \quad (2)$$

where k is the linear thermal expansion coefficient, and m is the slope of the transient line from the three points; (L_1, T_1), (L_2, T_2), (L_3, T_3).

Results and Discussion

Effect of LDPE on the Properties of the Wood-PVC Composites

Figure 1 illustrates the SEM micrograph of wood-PVC composites containing 0 to 40 phr polyethylene. The fracture

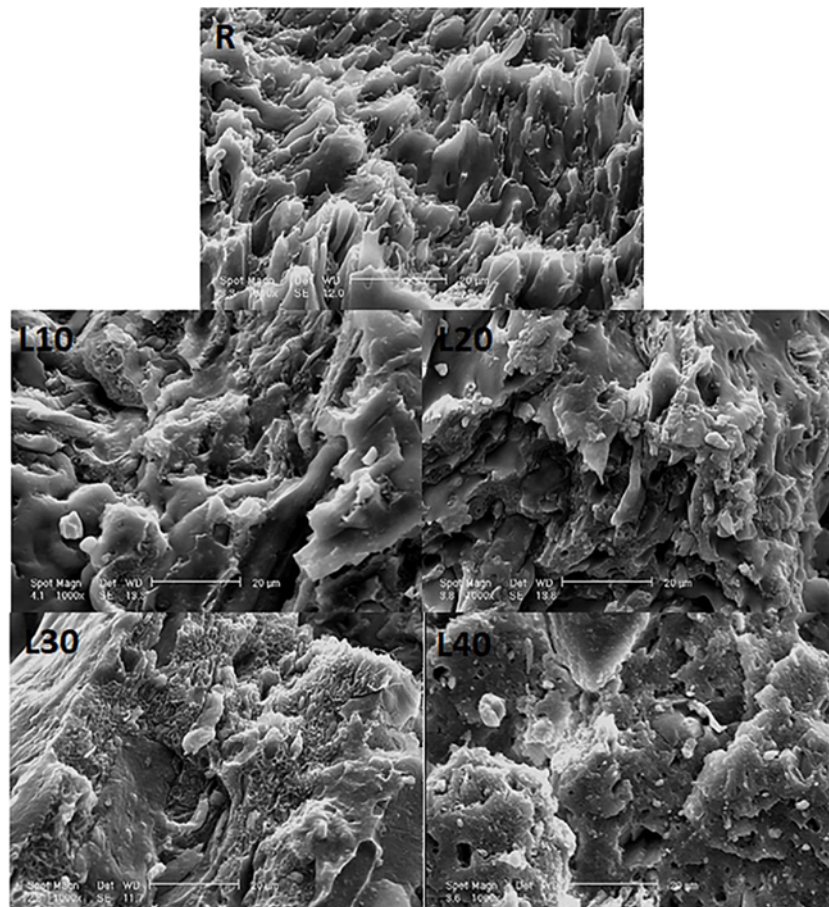


Figure 1. SEM micrograph of the wood-PVC composites with different LDPE contents.

Table 2. Mechanical and physical properties of wood-PVC/LDPE blend at different contents of LDPE

Sample code	Young's modulus (MPa)	Elongation at break (%)	Tensile strength (kPa)	Impact strength (kJ/m ²)	Water absorption (%)	Linear thermal expansion coefficient (1/°C)
R	45.062±7.9	6.17±0.2	254.84±15.75	2437.73±104.81	2.584±0.031	3.82×10 ⁻⁵
L10	186.785±6.6	6.64±0.2	236.39±4.04	2543.06±94.02	2.439±0.081	5.29×10 ⁻⁵
L20	168.843±6.3	7.06±0.3	217.67±9.65	2698.16±92.91	2.250±0.055	5.66×10 ⁻⁵
L30	124.786±6.5	8.77±0.2	199.11±14.98	2887.33±102.63	1.507±0.427	6.00×10 ⁻⁵
L40	109.016±6.9	8.97±0.2	175.06±15.44	2614.4±77.19	0.837±0.042	7.65×10 ⁻⁵

surface in all samples was rough, which indicates the proper adhesion between the polymer phase and wood particles. A droplet-matrix morphology in the fracture section was observed in the polyethylene- contained composites. The number and dimension of the droplets grow by increasing the amount of LDPE in the composition. Therefore, higher LDPE content in the composite resulted in weakening the interfacial adhesion.

To optimize the amount of LDPE in the composition, the mechanical, physical, and thermal properties of the wood-PVC/LDPE composites at different LDPE content (0 to 40 phr) were analyzed. As shown in Table 2, by the addition of 10 phr LDPE in the wood-PVC composite, the tensile modulus, and the elongation at break of the compound experienced the growth of about 75 % (P-value<0.05), and 8 % (P-value=0.5), respectively. While the ultimate tensile strength decreased about 7 % (P-value=0.01). Further increasing the amount of LDPE from 10 to 40 phr also decreased the UTS and the modulus of the compound (P-value<0.05). Young's modulus of the wood-PVC/LDPE composites reduced with increasing the LDPE content, due to the intrinsic properties of the LDPE in comparison to the rigid PVC [4]. Also, the poor interfacial adhesion between the blend components is the other reason for-decreasing the stiffness. Therefore, the phase of LDPE acts as a defect in the PVC matrix. A similar trend was also described by Prachayawarakorn *et al.* They found a reduction of 40 % in the tensile strength of the wood-PVC composite in the presence of 10 wt.% LDPE [5]. As can be noted in Table 2, the amount of LDPE in the composition had no significant effect on the impact strength of the composites (P-value>0.05). The composite containing 30 phr LDPE showed the highest amount of impact strength (about 15 % higher compared with the pure wood-PVC compound).

In similar research, Prachayawarakorn *et al.* investigated the effect of different compatibilizers and amounts of LDPE in the wood-PVC/LDPE composite. The results showed that using PA20 as a compatibilizer in presence of 50 phr sawdust and increasing the amount of LDPE from 10 to 40 phr resulted in a reduction of 61.5 % in Young's modulus, and 38.4 % in tensile strength with no change in impact strength of the composite. In the current research, with the

same compatibilizer (PA20) and more amount of sawdust (60 phr) the reduction of 41.5 % in Young's modulus (P-value=0.0001), and 25 % in the tensile strength (P-value=0.0006) with no significant change in impact strength (P-value=0.9) were observed in the LDPE/PVC blend. Therefore, the higher wood content (60 phr) can result in a lower reduction in mechanical properties. Besides, it can be a better choice for the environment and cost-saving.

It is noticeable that the tensile and impact properties of a composite are correlated to the compatibility of the different components. The presence of a coupling agent in the composition offers the improvement of the interfacial adhesion between the phases and therefore enhances the composite strength [4]. according to the recent study, using 15 % of the poly(methyl methacrylate-co-butyl acrylate) compatibilizer greatly enhanced the tensile strength, elongation at break, and impact strength of the PVC/LDPE (100/10) composite about 7 %, 80 %, and 34 %, respectively, compared to the uncompatibilized composite. In this research, MAPE with polar groups of anhydride along with PE nonpolar section was used as the coupling agent. The anhydride groups can make strong ester bonds with wood surfaces, and the nonpolar PE section can make physical entanglement with the LDPE, which is expected to increase the mechanical properties of the composite [13]. The schematic diagram of the chemical and physical interactions between the PVC/LDPE matrix along with wood particles in presence of the coupling agent and the compatibilizer is shown in Figure 2 [11]. The amount of the coupling agent in the composition is also an important parameter in defining the phase adhesion, and mechanical properties of the composite. The ratio of the MAPE to the LDPE was decreased from 18 % to 4.5 % with increasing the amount of LDPE from 10 to 40 phr in the composition. Therefore, reducing the ratio of the coupling agent to the LDPE caused the reduction of the mechanical strength of the composites. A similar tendency was also perceived in the SEM micrographs.

The outcomes of the water absorption of the composites are also represented in Table 2. Increasing the amount of polyethylene from 0 to 40 phr resulted in a reduction of the water absorption of the composites, which is due to the non-polar structure of polyethylene. It should be noted that water

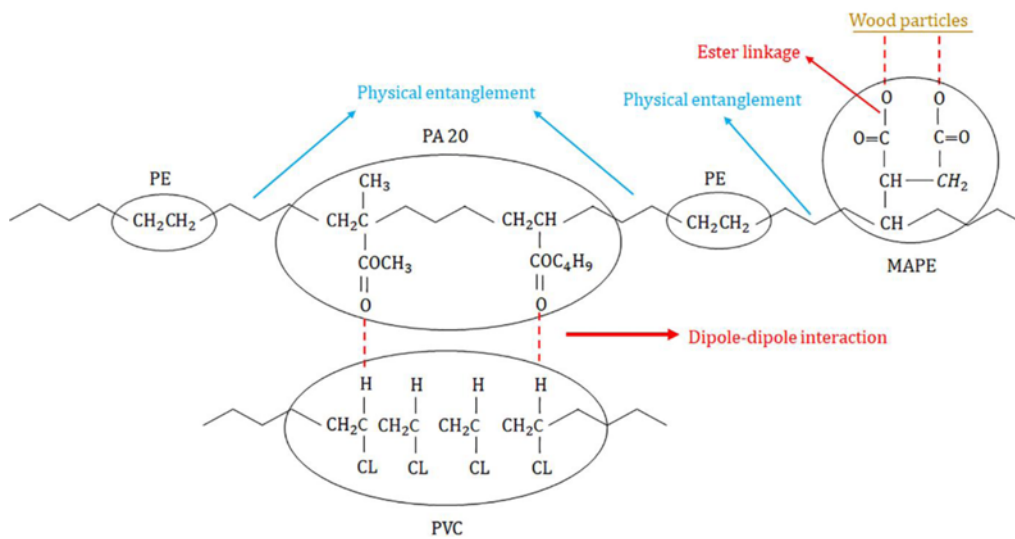


Figure 2. Schematic diagram of the chemical and physical interactions between the PVC/LDPE matrix along with wood particles in presence of the coupling agent, and the compatibilizer.

absorption of PVC is about 0.1 %, while polyethylene is nearly 0.01 %. Also, the R sample contained 34 wt.% of wood particles, whereas the amount of wood in the L40 sample was only 28 wt.%. Therefore, due to the high water absorption of wood particles (about 25 %), it was expected to observe the reduction of the water absorption in L30 and L40 compared to the R sample. Besides, the orientation of wood particles plays a vital role in the water absorption of the composite. The MAPE coupling agent in the composite encapsulates the wood particles with polyethylene chains and decreases the water absorption ability of the wood particles [29].

According to Table 2, increasing the amount of LDPE from 0 to 40 phr contributes to an increment in the linear thermal expansion coefficient of the composites. This behavior is because the linear thermal expansion coefficient of polyethylene is about 40 times higher than PVC [30]. Besides, the reduction of the weight ratio of wood particles in the composite with increasing the LDPE content increases this coefficient. A similar trend was observed by Wu *et al.* in WPCs based on HDPE [31].

According to the obtained results, the L30 sample with 30 phr LDPE was selected as an optimum compound for further investigation. The L30 sample showed the highest impact strength as 2887.33 kJ/m². The presence of LDPE in the composition decreased the tensile strength and increased the linear thermal expansion coefficient of the composite. The tensile strength and water absorption of the L30 sample dropped 21 (P-value=0.001), and 42 % (P-value=0.01) respectively, and the linear thermal expansion coefficient increased by 57 % compared with the R sample (P-value=0.01). To improve these properties, four contents of nanoclay were added to the L30 compound, in the next step.

Effect of Nanoclay on the Properties of the Wood-PVC/LDPE Composites

To improve the mechanical and thermal properties of the wood-PVC/LDPE composite, Cloisite 30B at four contents (1, 2, 3, and 4 phr) was added to the optimum compound. The XRD pattern of the nanoclay contained composites was illustrated in Figure 3. The XRD pattern of the pure Cloisite 30B shows a peak at $2\theta=4.38^\circ$ corresponding to 1.84 nm inter gallery distance [32]. The diffraction peak in the prepared composites with 1, 2, and 3 phr clay was disappeared, demonstrating the exfoliated structure of Cloisite 30B in these nanocomposites. The addition of the higher amount of nanoclay in the L30N4 sample shifted the diffraction peak to the lower degree, which is due to the formation of an intercalated structure in this nanocomposite [12]. Therefore, the polymer chains diffused between the layers of the nanoclay, forming the intercalated and exfoliated structures.

The effect of Cloisite 30B on the mechanical properties of the wood-PVC/30 phr LDPE was illustrated in Figure 4.

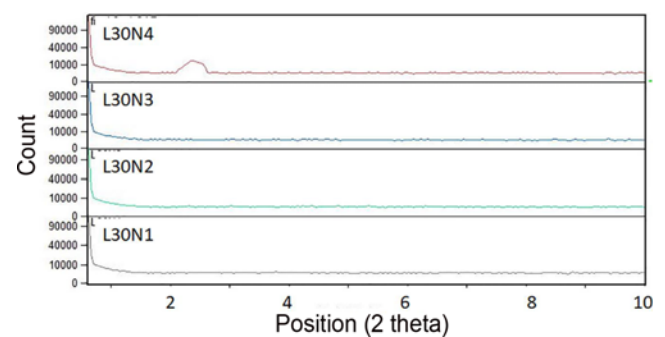


Figure 3. XRD patterns of the wood-PVC/LDPE composites containing 1 to 4 phr Cloisite 30B.

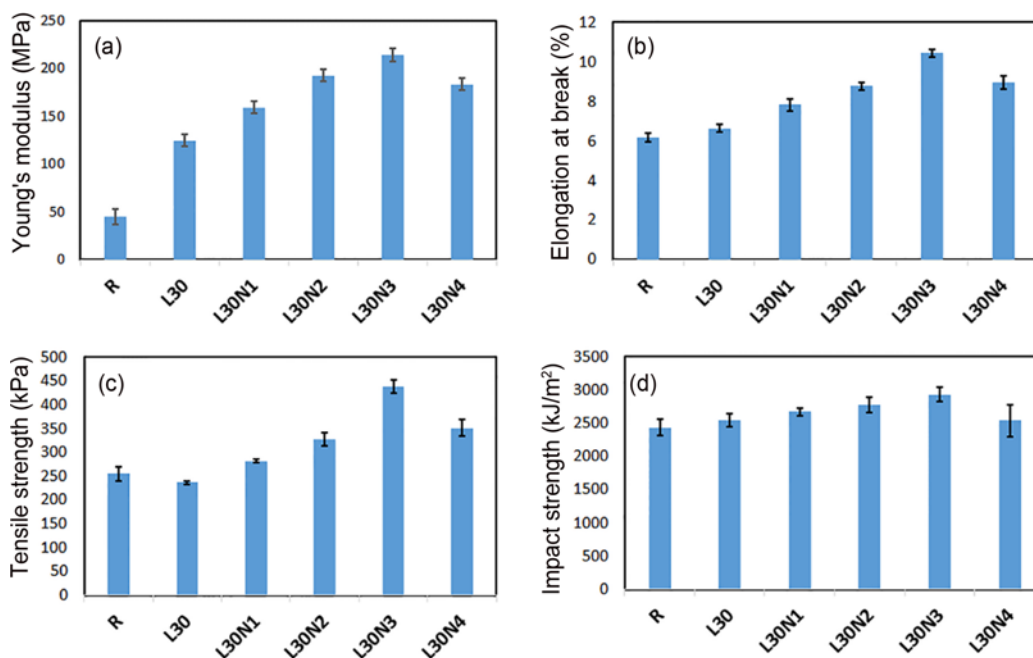


Figure 4. (a) Young’s modulus, (b) elongation at break, (c) tensile strength, and (d) impact strength of the wood-PVC/LDPE nanocomposites containing 0 to 4 phr Cloisite 30B.

Increasing the amount of nanoclay from 0 to 3 phr increased Young's modulus, elongation at break, and the ultimate tensile strength of the L30 compound, while further growing to 4 phr reduced these properties. However, the tensile strength value of the L30N4 compound was still higher than the L30 one. The agglomeration of the nanoclay in the interface of the wood and polymer is the reason for this decline in the mechanical properties. The high amount of wood particles in the composite decreases the reinforcement property of the nanoclay. A similar trend was seen in other researches [28,33]. Wu *et al.* showed that using 3 phr nanoclay in HDPE/Wood nanocomposites resulted in Young's modulus improvement of about 15.2 %, while in the current research, the enhancement of 70 % in the tensile modulus (P-value<0.05) was observed by adding 3 phr nanoclay [34]. The highest tensile strength value (438.36 kPa) was observed in the nanocomposite with 3 phr Cloisite 30B, which was 46 % higher than the L30 compound (P-value=0.02).

In order to calculate the number of stacks of the clay in the prepared nanocomposites, the tensile modulus data were inserted in the Halpin-Tsai equation [25].

$$\frac{E_{nanocomposite}}{E_{L30}} = \frac{1 + 2\alpha(N)\xi\phi}{1 - \xi\phi} \tag{3}$$

where $\alpha(N)$, and ζ come from $\alpha(N) = \frac{218}{N + (N-1)3.7}$, and $\xi = \frac{E_r - 1}{E_r + 2\alpha(N)}$, respectively. In equation (3), ϕ , and N are

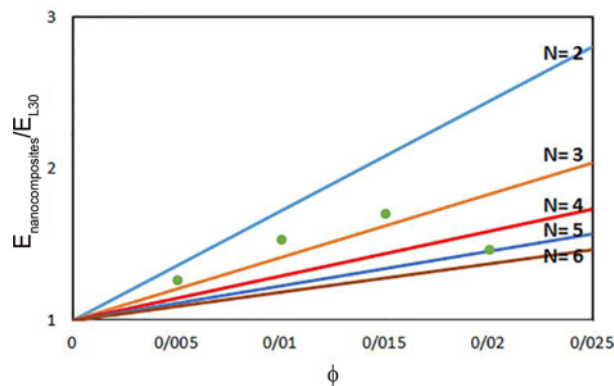


Figure 5. Modulus ratio of the nanocomposites to the L30 sample versus the volume fraction of the clay; predicted from the Halpin-Tsai equation for different clay stack numbers (N), along with the experimental data (●).

the volume ratio and the stack number of the clay. The amount of E_r obtains from the modulus ratio of the clay platelets (10^5 MPa) to the L30 matrix [25].

The amounts of the $E_{nanocomposites}/E_{L30}$ ratio for different stack numbers (N) from equation (3) are illustrated in Figure 5. The experimental values of the modulus ratio are also shown to predict the stack number of the clay in the prepared nanocomposites. As can be seen, the experimental modulus ratio for the nanocomposites containing up to 3 phr nanoclay placed between the theoretical lines of two and three. However, increasing the clay content to 4 phr ($\phi=0.02$)

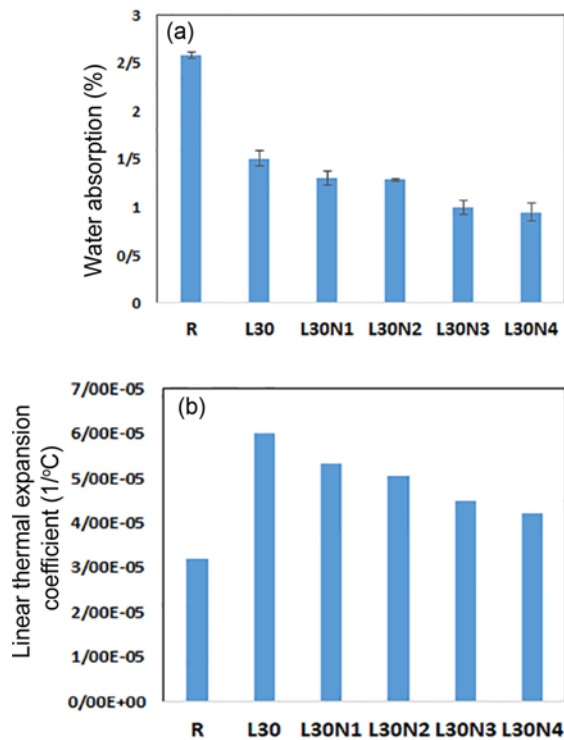


Figure 6. (a) The water absorption and (b) the linear thermal expansion coefficient of the wood-PVC/LDPE nanocomposites containing 0 to 4 phr Cloisite 30B.

increased the stack number to about five. Therefore, the aggregation of the clay platelets resulted in the decline of the mechanical properties of the L30N4 sample.

Figure 4(d) presents the impact strength of the wood-PVC/LDPE composites in the various amounts of the nanoclay. The effect of the nanoclay content on the impact strength was similar to the tensile strength of the composites. The impact strength of the compounds was improved by the addition of 1 to 3 phr nanoclay, while the presence of more nanoclay resulted in reducing the impact strength. According to Figure 4(d), the L30N3 has the highest impact strength of about 14 % higher than the R sample. It can be related to the exfoliated structure, and appropriate dispersion of the nanoclay in this composite, which leads to better stress transfer from the polymer matrix to the particles, and thereby higher energy is required for the composite failure [35].

Figure 6(a) illustrates the water absorption percentage of the prepared nanocomposites. The results showed that the presence of the nanoclay decreased the water absorption of the wood-PVC/LDPE nanocomposites. The reduction of water absorption was intensified in more nanoclay content. The layer structure of clay complicates the water transfer pathway and thus reduces the water diffusion coefficient. Besides, As the clay content increases in the composite, the holes in the wood particles, which trap water molecules, are occupied by the nanoparticles and polymer chains. These

two phenomena decrease the water absorption capacity of the nanocomposite. Other researchers also reported similar results in different nanocomposites [12,28,34]. Wu *et al.* revealed that using 3 phr nanoclay in the HDPE/clay/wood nanocomposites declined the water absorption by about 22 % after 10 days, however in our research, enhancement higher decrease of 34 % in the water absorption was observed only after 24 hours immersion [34].

The linear thermal expansion coefficients of the wood-PVC/LDPE nanocomposites in the various contents of Cloisite 30B are shown in Figure 6(b). The results displayed the reduction of the linear thermal expansion coefficient by using the nanoclay in the composition. Therefore, the thermal stability of the nanocomposites was improved in the presence of the nanoclay. Zhong *et al.* observed that the addition of up to 3 phr nanoclay can develop the thermal property of the composite, while further increasing can show worse effect due to the agglomeration of the nanoclay in the structure. They reported the maximum improvement of about 56 % in the thermal property by using 3 phr nanoclay in the composite [23]. In our study, the maximum reduction of the linear thermal expansion coefficient was also detected in the nanocomposite with 3 phr Cloisite 30B, which was 25 % lower than the L30 compound.

Conclusion

Firstly, the effect of LDPE content on the morphology, mechanical, physical, and thermal properties of the wood-PVC/LDPE composites was investigated. Increasing the amount of LDPE from 0 to 40 phr decreased the phase adhesion, and thereby the tensile strength of the composite. The presence of LDPE in the composition reduced the water absorption, and increased the linear thermal expansion coefficient of the composite. According to the obtained results, the wood-PVC composite with 30 phr LDPE was selected as an optimum compound for further investigation. The mentioned composite showed the highest impact strength as 2887.33 kJ/m². In the next step, the effect of adding 0 to 4 phr nanoclay on the mechanical, physical, and thermal properties of the optimum composite was considered. The XRD pattern of the nanocomposites confirmed the exfoliated structure at clay content up to 3 phr, and intercalated configuration at 4 phr Cloisite 30B. The presence of the nanoclay improved the tensile properties and impact strength of the nanocomposites. Increasing the Cloisite 30B content declined the water absorption and the linear thermal expansion coefficient of the composite. The overall results introduced the composition of 100 phr PVC with 60 phr wood, 30 phr LDPE, and 3 phr Cloisite 30B with appropriate properties. The tensile strength, impact strength, water absorption, and the linear thermal expansion coefficient of this composite were measured as 438.36 kPa, 2932.2 kJ/m², 1 %, and 4.5×10⁻⁵ 1/°C, respectively.

Conflict of Interest

The authors declare that they have no known competing financial interests or personal relationships that could have appeared to influence the work reported in this paper.

References

1. S. Maou, A. Meghezzi, N. Nebbache, and Y. Meftah, *J. Vinyl. Addit. Technol.*, **25**, E88 (2019).
2. B. Kord, A. Varshoei, and V. Chamany, *J. Reinf. Plast. Comp.*, **30**, 1115 (2011).
3. B. Kord, P. Ravanfar, and N. Ayrilmis, *J. Polym. Environ.*, **25**, 1198 (2017).
4. A. Vedrtnam, *Compos. Commun.*, **8**, 31 (2018).
5. J. Prachayawarakorn, J. Khamsri, K. Chaochanchaikul, and N. Sombatsompop, *J. Appl. Polym. Sci.*, **102**, 598 (2006).
6. M. Jahadi, S. N. Khorasani, and M. Palhang, *J. Appl. Polym. Sci.*, **119**, 2627 (2011).
7. A. Vedrtnam and D. Gunwant, *Mater. Res. Express*, **6**, 105408 (2019).
8. S.-M. Lai, F.-C. Yeh, Y. Wang, H.-C. Chan, and H.-F. Shen, *J. Appl. Polym. Sci.*, **87**, 487 (2003).
9. F. Zhang, W. Qiu, L. Yang, T. Endo, and T. Hirotsu, *J. Appl. Polym. Sci.*, **89**, 3292 (2003).
10. N. Sombatsompop, C. Yotinwattanakumtorn, and C. Thongpin, *J. Appl. Polym. Sci.*, **97**, 475 (2005).
11. A. Espert, W. Camacho, and S. Karlson, *J. Appl. Polym. Sci.*, **89**, 2353 (2003).
12. C. Esnaashari, S. N. Khorasani, M. Entezam, and S. Khalili, *J. Appl. Polym. Sci.*, **127**, 1295 (2013).
13. J. Prachayawarakorn, S. Khunsumled, C. Thongpin, A. Kositchaiyong, and N. Sombatsompop, *J. Appl. Polym. Sci.*, **108**, 3523 (2008).
14. L. M. Matuana, D. P. Kamdem, and J. Zhang, *J. Appl. Polym. Sci.*, **80**, 1943 (2001).
15. N. Sombatsompop and K. Chaochanchaikul, *J. Appl. Polym. Sci.*, **96**, 213 (2005).
16. C. Thongpin, O. Santavitee, and N. Sombatsompop, *J. Vinyl. Addit. Technol.*, **12**, 115 (2006).
17. C. Xu, Z. Fang, and J. Zhong, *Die Angewandte Makromolekulare Chemie*, **212**, 45 (1993).
18. A. Vedrtnam, S. Kumar, and S. Chaturvedi, *Compos. B. Eng.*, **176**, 107282 (2019).
19. Y. Geng, K. Li, and J. Simonsen, *J. Appl. Polym. Sci.*, **99**, 712 (2006).
20. C. Zhang, K. Li, and J. Simonsen, *Polym. Eng. Sci.*, **46**, 108 (2006).
21. J. Z. Lu, Q. Wu, and I. I. Negulescu, *J. Appl. Polym. Sci.*, **96**, 93 (2005).
22. Y. Geng, K. Li, and J. Simonsen, *J. Appl. Polym. Sci.*, **91**, 3667 (2004).
23. Y. Zhong, T. Poloso, M. Hetzer, and D. De Kee, *Polym. Eng. Sci.*, **47**, 797 (2007).
24. A. Rouhollahi, S. N. Khorasani, A. Farzadfar, S. Khalili, and M. Asgari, *J. Appl. Polym. Sci.*, **131**, 40150 (2014).
25. S. Khalili, M. Masoomi, and R. Bagheri, *J. Plast. Film. Sheeting*, **29**, 39 (2013).
26. Y. Zhao, K. Wang, F. Zhu, P. Xue, and M. Jia, *Polym. Degrad. Stab.*, **91**, 2874 (2006).
27. S. Borysiak, D. Paukszta, and M. Helwig, *Polym. Degrad. Stab.*, **91**, 3339 (2006).
28. B. Deka and T. K. Maji, *Compos. Sci. Technol.*, **70**, 1755 (2010).
29. A. A. Klyosov, "Wood-Plastic Composites", pp.161-201, John Wiley & Sons, Inc., New Jersey, 2007.
30. Awwa Manual, "Pvc Pipe-design and Installation", 2nd Ed., American Water Works Association, 2002.
31. Q. Wu, K. Chi, Y. Wu, and S. Lee, *Mater. Des.*, **60**, 334 (2014).
32. K. T. Hafshejani, S. N. Khorasani, M. Jahadi, M. S. Hafshejani, and R. E. Neisiany, *J. Therm. Anal. Calorim.*, **137**, 175 (2019).
33. H. Lee and D. S. Kim, *J. Appl. Polym. Sci.*, **111**, 2769 (2009).
34. Q. Wu, Y. Lei, F. Yao, Y. Xu, and K. Lian, 2007 First International Conference on Integration and Commercialization of Micro and Nanosystems, pp.181-188, 2007.
35. M. Saeedi, I. Ghasemi, and M. Karrabi, *Iran. Polym. J. (English)*, **20**, 131 (2011).